Measurement of the Pion Form Factor*

C. W. AKERLOF,† W. W. ASH, K. BERKELMAN,‡ C. A. LICHTENSTEIN, A. RAMANAUSKAS, AND R. H. SIEMANN
Laboratory of Nuclear Studies, Cornell University, Ithaca, New York
(Received 5 July 1967)

Cross sections for the electroproduction reaction $e+p \rightarrow e+n+\pi^+$ have been measured at invariant momentum transfers $k^2=-1, -3, -6$ F^{-2}. The circulating beam of the Cornell 2-GeV electron synchrotron struck a liquid-hydrogen target mounted in the synchrotron vacuum chamber in a field-free section between ring magnets. Pions produced along the momentum-transfer direction were counted in coincidence with inelastically scattered electrons. Both were momentum analyzed by quadrupole magnets and detected in scintillation counters and (for the electrons) a shower Čerenkov counter. The effective mass of the final pion-nucleon system was varied from 1175 to 1300 MeV. The relative contribution of transverse and longitudinal photon exchanges was varied by changing the electron scattering angle. Electroproduction yields were normalized to elastic cross sections measured with the same electron spectrometer at the same incident energy. The eight measured cross sections have been compared with recent dispersion calculations. The agreement is very sensitive to the value chosen for the pion charge form factor, the only free parameter in the theory. Taking into account both experimental errors (typically 10% in the cross sections) and estimates of the reliability of the theory (also around 10%) based on comparison with other experiments, the following results were obtained: $F_\pi(-1\text{ F}^{-2})=0.79_{-0.18}{}^{+0.16}$, $F_\pi(-3\text{ F}^{-2})=0.82\pm0.06$, and $F_\pi(-6\text{ F}^{-2})=0.57_{-0.09}{}^{+0.08}$. Within the errors, the pion and proton charge form factors are identical. The pion form factor is also reasonably consistent with the ρ-exchange model: $F_\pi=(1-k^2/m^2)^{-1}$ with $m=600\pm80$ MeV. The root-mean-square charge radius of the pion is $r_\pi=(\sqrt{6})/m=0.80\pm0.10$ F.

I. INTRODUCTION

In this paper we shall take the term electroproduction to mean single-pion production by inelastic scattering of electrons on protons; that is, we consider the reactions $e+p \rightarrow e+p+\pi^0$ and $e+p \rightarrow e+n+\pi^+$. Electroproduction can be thought of as a generalization of elastic scattering, $e+p \rightarrow e+p$, or in terms of the photoproduction reactions $\gamma+p \rightarrow p+\pi^0$ and $\gamma+p \rightarrow n+\pi^+$. The electroproduction yield as a function of the invariant electron momentum transfer depends on the electromagnetic form factors of the hadrons involved in the reaction, just as in the case of elastic scattering; while the pion angular distribution and the dependence of the yield on the hadron final-state center-of-mass energy share the same features displayed in the photoproduction data. Many of the conclusions which have been drawn from elastic scattering and photoproduction data can be checked in electroproduction: the momentum-transfer dependence of the nucleon form factors, the energies, widths, and photoexcitation strengths of nucleon resonances, and so on. There are, however, important physical quantities which can be measured only through electroproduction. One of these is the charge form factor of the pion. We report here the results of an experimental investigation of electroproduction designed to measure the pion form factor.[1] First, however, we survey the historical development of electroproduction and review its connection with photoproduction.

The first experimental observation of the electroproduction of pions was made by Panofsky, Woodward, and Yodh.[2] They measured the yield of positive pions produced in a proton target by the incident electron beam. However, since fixing the incident electron and final pion momenta does not fix the electron momentum transfer either in direction or magnitude, the data were of marginal use in extracting information about the details of the interaction.

In later experiments Panofsky and his collaborators[3] detected instead the inelastically scattered electron to get a measure of the total π^+ and π^0 electroproduction at fixed values of the momentum transfer and pion-nucleon center-of-mass energy. This type of experiment is very useful for preliminary exploration of nucleon resonances and can be used to obtain information on the momentum-transfer behavior of the effective resonance excitation form factors in favorable cases where the resonance amplitude is clearly resolved from other resonances and the nonresonant background; however, a detailed comparison with theoretical models is possible only if one knows the relative contributions of the various meson charge states and their angular distributions. This requires simultaneous detection of the scattered electron and the pion (or nucleon, whichever is easier).

* Work supported by the National Science Foundation.
† Present address: Physics Department, University of Michigan, Ann Arbor, Michigan.
‡ On leave 1967–68 at CERN, Geneva, Switzerland.
[1] A preliminary report has already been published: C. W. Akerlof, W. W. Ash, K. Berkelman, and C. A. Lichtenstein, Phys. Rev. Letters **16**, 147 (1966). The present report is based on about three times as much data and a refined analysis.
[2] W. K. H. Panofsky, W. M. Woodward, and G. B. Yodh, Phys. Rev. **102**, 1392 (1956). A more recent version of this experiment is reported by S. P. Berezin, P. C. Gugelot, and P. Heide, in *Proceedings of the International Symposium on Electron and Photon Interactions at High Energies, Hamburg, 1965*, edited by G. Höhler *et al.* (Deutsche Physikalische Gesellschaft, Hamburg, 1965), Vol. II. p. 269.
[3] W. K. H. Panofsky and E. A. Allton, Phys. Rev. **110**, 1155 (1958); G. G. Ohlsen, *ibid.* **120**, 584 (1960); L. N. Hand, *ibid.* **129**, 1834 (1964). Recent work at higher energies has been reported by A. A. Cone, K. W. Chen, J. R. Dunning, G. Hartwig, N. F. Ramsey, J. K. Walker, and R. Wilson, *ibid.* **156**, 1490 (1967).

The coincidence experiment is very much more difficult because: (1) relative to the total inelastic yield the coincidence counting rate is reduced by a factor proportional to the fraction of the full solid angle subtended by the pion detector, and (2) the singles rates in both the electron and pion detectors are very much larger than the coincidence rate, so that accidental coincidences can make it impossible to use enough beam flux to overcome the first difficulty. The first attempt to measure π^0 electroproduction by observing electron-proton coincidences was reported by Perez y Jorba, Bounin, and Chollet,[4] while the first measurements of $e\pi^+$ coincidences were made by Akerlof, Ash, Berkelman, and Tigner.[5] Both of these experiments were severely limited by accidental coincidences, the first because the electron beam from the Orsay linear accelerator has only a 10^{-4} duty factor, and the second because the pions were detected without momentum analysis. The present experiment has neither of these defects.

Frazer[6] has suggested that the pion form factor can be determined from π^+ electroproduction data. The dependence on F_π comes in the one-pion-exchange pole diagram [Fig. 1(c)], which can be viewed as the elastic scattering of an electron off a virtual π^+ emitted by the target proton. To isolate this amplitude from the others which tend to mask its effect, Frazer proposed an extrapolation of pion angular-distribution data to the pole at $(p_\mu - p_\mu')^2=\mu^2$, which occurs at an unphysical pion angle. To obtain a pion angular distribution at fixed momentum transfer and pion-nucleon center-of-mass energy the experimenter must of course detect both the electron and the π^+. Without a model for the other amplitudes a successful extrapolation requires a degree of accuracy in the data which is beyond present experimental capabilities. Alternatively, if one has an adequate theory for the complete electroproduction amplitude, and if one can find energies and angles at which the pion pole term makes a large contribution, one can directly fit experimental data to the theory to determine the unknown pion form factor. This puts much less burden on the experimenter, but of course, any conclusions about the pion form factor become very sensitive to shortcomings of the theoretical model used in the fitting. Nevertheless, we have chosen this method as the only practical way at present of getting the pion form factor from electroproduction, and we have attempted to test the theoretical model in as many ways as possible and evaluate the effect of any discrepancies.

II. ELECTROPRODUCTION PHENOMENOLOGY

We will use the following notation for the kinematic variables involved in the electroproduction reaction: The laboratory-frame momentum four-vectors of the incident and scattered electron, the target and final nucleon, and the electroproduced pion are r_μ, r_μ', p_μ, p_μ', and q_μ, respectively (see also Fig. 1). The corresponding variables evaluated in the center-of-mass frame of the final-state pion and nucleon are represented by the corresponding capital letters. The masses of electron, proton, and pion are denoted by m, M, and μ. The metric we use is specified by $r_\mu^2=r_0^2-\mathbf{r}^2=m^2$, and so on. It will be convenient to define two invariants. The first is the square of the four-momentum transferred by the scattered electron to the hadron system, defined as follows:

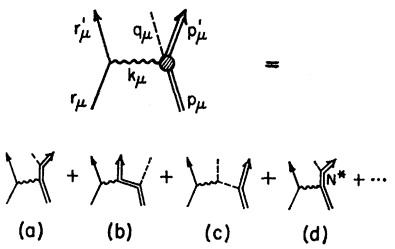

FIG. 1. Diagrams representing various contributions to the electroproduction amplitude.

$$\begin{aligned} k^2 &= k_0^2-\mathbf{k}^2 \text{ (lab frame)} \\ &= K_0^2-\mathbf{K}^2 \ (\pi N \text{ center-of-mass}) \\ &= k_\mu^2=(r_\mu-r_\mu')^2. \end{aligned}$$

It is negative in electroproduction.[7] If we neglect the mass of the electron, taking $|\mathbf{r}|=r_0=E$ and $|\mathbf{r}'|=r_0'=E'$, we have the following expression for k^2 in terms of the laboratory energies and scattering angle θ_e:

$$k^2=-2EE'(1-\cos\theta_e). \tag{1}$$

The second invariant is given by

$$W^2=(p_\mu'+q_\mu)^2.$$

W is the total energy of the final nucleon and pion in the frame in which their combined momentum is zero; that is, $W=P_0'+Q_0$. If the pion and nucleon are thought of as decay products of a single particle state, W is the mass of that state. W is also determined by the incident and scattered electron energies and the lab scattering angle:

$$W^2=M^2+k^2+2M(E-E'). \tag{2}$$

It is important to recognize that k^2 and W are independent variables; for any θ_e one can choose E and E' to give any k^2, W combination (see Fig. 2).

The representation of the elastic electron-proton scattering in terms of proton form factors is based on two important hypotheses: (1) that conventional quantum electrodynamics correctly describes the behavior of the electron and the electromagnetic field, and (2) that a single photon[8] is exchanged (see Fig. 1). The first as-

[4] J. P. Perez y Jorba, P. Bounin, and J. Chollet, Phys. Letters **11**, 350 (1964).
[5] C. W. Akerlof, W. W. Ash, K. Berkelman, and M. Tigner, Phys. Rev. Letters **14**, 1036 (1965).
[6] W. R. Frazer, Phys. Rev. **115**, 1763 (1959).

[7] Here, k^2 has the same meaning as $-q^2$ in the elastic electron scattering literature. Our notation is closer to that common in the photoproduction literature.
[8] The radiative correction accounts for the effects of multiple photon exchange only in the soft-photon limit.

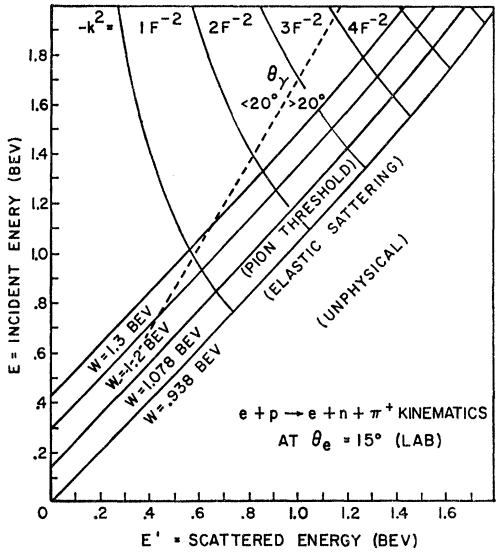

FIG. 2. A plot of W and k^2 as functions of the incident and scattered energies E and E' at fixed scattering angle [Eqs. (1) and (2)].

sumption has been tested in elastic electron-electron scattering,[9] and less directly in other high-energy electromagnetic processes.[10] Loosely speaking, the result can be stated in terms of a maximum size of about 0.5 F for the electron. There is no convincing evidence of a deviation from the quantum electrodynamics of point electrons.

The consequences of the single-photon-exchange assumption have been experimentally checked[10] in the scattering angular distribution at fixed momentum transfer, in the recoil proton polarization, and in the equality of e^-p and e^+p scattering cross sections. Although not one of these experiments is sensitive enough to rule out a small multiple-photon contribution, no such effect has been seen up to momentum transfers of about 1 $(\mathrm{GeV}/c)^2$.

Our analysis of electroproduction (see Appendix I for details) will be based on the same two hypotheses, although neither has been tested in electroproduction. The four-momentum k_μ given up by the electron is carried by a single photon (Fig. 1). The electron-photon vertex and photon propagator are known from quantum electrodynamics; the photon-hadron vertex is like pion photoproduction. There are three important differences, however, between this virtual photoproduction reaction and the usual photoproduction by real photons in a bremsstrahlung beam. First, these photons are spacelike, off the mass shell by the amount given by the electron momentum transfer k^2 (negative). Secondly, when the scattered electron is detected at a fixed angle and momentum, the corresponding photon is monenergetic. A useful measure of its energy is the center-of-mass energy W in the resulting virtual photoproduction reaction. And finally, the virtual photon is polarized, longitudinally as well as transversely. The photon is in an incoherent mixture of two pure polarization states (see Appendix I), one normal to the scattering plane (the y axis) and therefore transverse, the other in the plane partly transverse (the x axis) and partly longitudinal (z axis). In the pion-nucleon center-of-mass frame the two vectors are [Eq. (A10)]

$$\begin{pmatrix} 0 \\ [\frac{1}{2}(1-\epsilon)]^{1/2} \\ 0 \end{pmatrix} \quad \text{and} \quad \begin{pmatrix} [\frac{1}{2}(1+\epsilon)]^{1/2} \\ 0 \\ \epsilon^{1/2} \end{pmatrix}.$$

The polarization parameter ϵ is defined by

$$\epsilon=[1+2(|\mathbf{k}|^2/|k^2|)\tan^2(\tfrac{1}{2}\theta_e)]^{-1}, \qquad (3)$$

and is a measure of both the transverse and longitudinal polarization. It is determined by the electron kinematic variables E, E', and θ_e, but is most strongly dependent on angle, varying from essentially 100%[11] at forward angles to zero for backward scattering (see Fig. 3).

The three laboratory kinematic variables E, E', and θ_e, fixed by detecting the scattered electron, can then be mapped into the three variables k^2, W, and ϵ, which are more relevant to the theoretical interpretation. However, the differential cross section for a process of the type $a+b\rightarrow c+d+e$ (such as electroproduction) is in principle a function of five independent variables, pro-

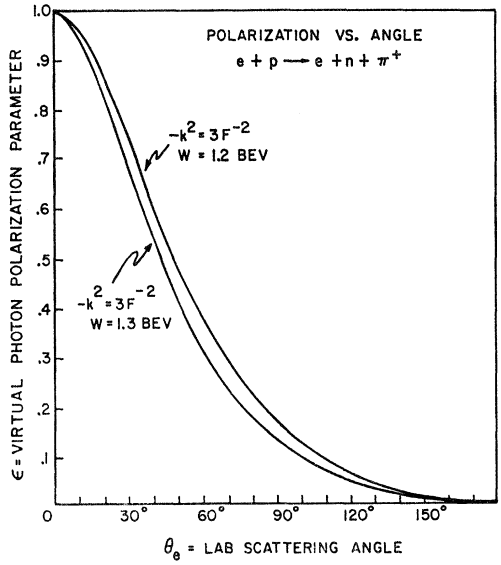

FIG. 3. The photon-polarization parameter as a function of the lab-electron scattering angle for several values of W and k^2 [Eq. (3)].

[9] W. C. Barber, B. Gittelman, G. K. O'Neill, and B. Richter, Phys. Rev. Letters **16**, 1127 (1966).

[10] S. D. Drell, in *Proceedings of the Thirteenth International Conference on High-Energy Physics, Berkeley, California, 1966*, edited by M. Alston-Garnjost (University of California Press, Berkeley, California, 1967), p. 85.

[11] Although the polarization given by (3) is apparently 100% at $\theta_e=0$, this is only a consequence of neglecting the electron mass. At extremely small angles polarization effects actually go to zero, as they should.

vided one does not specify the spins of the particles a, b, c, d, and e. We have accounted for three variables already; the remaining two specify the direction of emission of the pion. It will be convenient to define this direction with respect to the direction **K** of the virtual photon, and measure angles in the photoproduction center-of-mass frame. The polar angle between the pion momentum **Q** and the photon momentum **K** we denote by Θ_π, and the corresponding azimuth by ϕ (see Fig. 4).

We specify the yield of pion electroproduction in terms of the differential cross section $d\sigma/dE'd\omega_e d\Omega_\pi$, where $d\omega_e$ is the scattered-electron solid-angle differential in the laboratory and $d\Omega_\pi$ is the pion solid-angle differential measured in the center-of-mass frame of the final pion and nucleon. We can express the electroproduction cross section in terms of an effective center-of-mass differential cross section for virtual photoproduction [see Eq. (A7)]:

$$\frac{d\sigma}{dE'd\omega_e d\Omega_\pi}=\frac{\alpha}{2\pi^2}\frac{E'}{E}\frac{|\mathbf{k}|}{|k^2|}\frac{1}{1-\epsilon}\frac{d\sigma_v}{d\Omega_\pi}(W,k^2,\epsilon,\Theta_\pi,\phi). \quad (4)$$

The effects of the electron-photon vertex and the photon propagator are contained in the electrodynamics factor

$$\frac{\alpha}{2\pi^2}\frac{E'}{E}\frac{|\mathbf{k}|}{|k^2|}\frac{1}{1-\epsilon},$$

which can be interpreted as the number of virtual photons per electron scattered into dE' and $d\omega_e$. The factor $d\sigma_v/d\Omega_\pi$ is the center-of-mass differential cross section for pion photoproduction by virtual photons polarized as discussed above.

The polarization is manifest in the pion angular distribution. The general form[12] of the virtual-photon cross section (see Appendix I) is given by

$$d\sigma_v/d\Omega_\pi=A(W,k^2,\Theta_\pi)+\epsilon B(W,k^2,\Theta_\pi)+\epsilon C(W,k^2,\Theta_\pi)\sin^2\Theta_\pi\cos2\phi+[\epsilon(1+\epsilon)]^{1/2}D(W,k^2,\Theta_\pi)\sin\Theta_\pi\cos\phi. \quad (5)$$

The explicit dependence on ϵ and ϕ is a consequence of the single-photon-exchange hypothesis and the spin and parity of the photon. The first term A is the differential cross section for unpolarized transverse virtual photons. In the $k^2=0$ limit it approaches the ordinary real photoproduction cross section $d\sigma(W,\Theta_\pi)/d\Omega_\pi$. The third term $\epsilon C\sin^2\Theta_\pi\cos2\phi$ is the modification to the cross section due to the transverse linear polarization, hence the factor of ϵ and the azimuthal variation. It arises from the interference between $+1$ and -1 photon helicity amplitudes. In the $k^2=0$ limit it approaches the corresponding term in the cross section for photoproduction by real linearly polarized photons. The second term ϵB is the longitudinal contribution, with B representing the cross section for photoproduction by a pure longitudinal beam. It vanishes, of course, for real photons ($k^2=0$). The last term in (5) arises from the interference between transverse and longitudinal amplitudes. The four functions A, B, C, and D can be obtained separately from experiment. The two interference terms, involving C and D, can be identified by their characteristic azimuthal dependences.[5] The pure transverse and longitudinal terms, A and ϵB, are distinguished by their dependence on photon polarization, which is mainly a function of the electron angle θ_e.

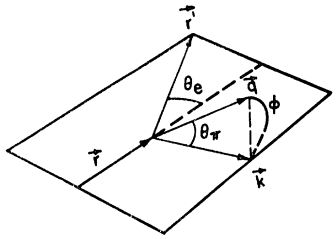

FIG. 4. Diagram in the laboratory frame illustrating the definition of the momentum vectors and angles.

If the pion (or recoil nucleon) is not detected, the measured electroproduction cross section becomes an integral over pion directions, in which case the interference terms disappear in the integral over ϕ, and we have the familiar[3] formula for the total virtual photoproduction cross section:

$$\sigma_v=\sigma_T(W,k^2)+\epsilon\sigma_L(W,k^2),$$

where

$$\sigma_T=\int A\,d\Omega_\pi \quad \text{and} \quad \sigma_L=\int B\,d\Omega_\pi.$$

Although σ_v is rather insensitive to the charge form factor of the pion, it is possible to find energies and angles for which $d\sigma_v/d\Omega_\pi$ has an enhanced sensitivity to F_π. Some of the more important amplitudes contributing to π^+ electroproduction are illustrated in Fig. 1. The same diagrams occur in π^0 production except that for neutral pions the pole term (1c) is absent[13] and the nucleon and crossed-nucleon pole terms (1a and 1b) partially cancel. In either case the dominant contribution to the cross section for $W<1300$ MeV is the production of the $N^*(1230)$ resonant state (1d). This state can in principle be reached by absorption of a magnetic dipole, transverse electric quadrupole, or longitudinal electric quadrupole photon. Symmetry schemes such as $SU(6)_W$ [14] and the quark model[15] predict that both of the electric quadrupole amplitudes are zero, and the photoproduction data[16] confirm that the transverse electric quadrupole amplitude is very small. The conclusion then is that the resonance contributes only to the transverse part of the cross section.

[12] We have changed the notation somewhat from that used in Refs. 1 and 5.

[13] The charge form factor of the π^0 must be identically zero for all k^2, since the π^0 is its own charge conjugate.

[14] H. Harari and H. J. Lipkin, Phys. Rev. **140**, 1617 (1965).

[15] C. Becchi and G. Morpurgo, Phys. Letters **17**, 352 (1965).

[16] M. Gourdin and P. Salin, Nuovo Cimento **27**, 193 (1963); D. J. Drickey and R. F. Mozely, Phys. Rev. Letters **8**, 291 (1962).

The pion pole amplitude contains the factor $[(p_\mu - p_\mu')^2 - \mu^2]^{-1}$, which in the $k^2=0$ limit is proportional to $(1-\beta_\pi \cos\Theta_\pi)^{-1}$. The pole occurs at the unphysical angle $\cos\Theta_\pi = 1/\beta_\pi$; and the corresponding amplitude in the physical region should reach its maximum at $\Theta_\pi = 0$, that is, for **Q** parallel to **K**. The transverse contribution, however, never reaches this maximum because it actually vanishes at $\Theta_\pi = 0$ by angular-momentum conservation. A transverse photon has one unit of spin angular momentum parallel or antiparallel to its motion (the z axis), but a pion moving in the same direction has $J_z = L_z = 0$. The only way a transverse photon can produce a forward pion is by flipping the spin of the nucleon, which it cannot do in the pion-exchange process. A longitudinal photon has no helicity to get rid of, so the longitudinal pion pole amplitude actually does attain its maximum in the forward direction.

It appears then that the elusive pion pole amplitude should stand out best above the resonance background in the longitudinal part (ϵB) of the cross section and at an angle $\Theta_\pi = 0$. At this pion angle the interference terms in the virtual photoproduction vanish, and we have simply

$$d\sigma_v(\Theta_\pi = 0)/d\Omega_\pi = A(W,k^2,0) + \epsilon B(W,k^2,0). \quad (6)$$

The longitudinal contribution is maximized relative to the transverse by chosing as small an electron angle θ_e as possible, thus giving a polarization ϵ close to 100% (see Fig. 3). This fortunately maximizes the electroproduction yield because of the presence of the factor $(1-\epsilon)^{-1}$ in Eq. (4).

The plan of the experiment was, therefore, to measure the $e\pi^+$ coincidence rate at various values of k^2, W, and ϵ, keeping Θ_π fixed at zero.

III. APPARATUS

A. Beam

The incident electrons for this experiment were provided by the circulating beam of the Cornell 2-GeV electron synchrotron. At the peak of the acceleration cycle a distortion was made in the beam orbit by exciting perturbing fields in two of the synchrotron ring magnets, causing the beam to pass through a target placed in the synchrotron vacuum chamber. Most electrons passed through the target several times before suffering enough energy loss or accumulating enough of a scattering angle to leave a stable orbit. The actual number of traversals depended on the beam energy, orbit aperture, target material, thickness, and position; typically, electrons at 1 GeV circulated until they had passed through about 0.01 radiation length.

The maximum number of electrons accelerated in this experiment was about 10^{10} per cycle, at a repetition rate of 30 cps. The energy was monitored by electronically integrating the voltage across the synchrotron magnet coils from injection time to the peak of the acceleration cycle. The energy stability of the synchrotron was good to about ± 5 MeV. The calibration was uncertain by no more than 5 MeV.

At high energies the beam spot as it first hits the target is likely to be extremely well defined; but because of multiple traversals it was spread out to about 2-mm diam, as judged from target radiation damage. The time distribution of the beam spill on the target was approximately Gaussian with a full width at half-maximum of about 0.7 msec, corresponding to a beam duty cycle of about 2%. The energy variation during the spill time was less than 1 MeV.

B. Target

The target was liquid hydrogen contained in a 1.3-cm-diam vertical cylinder of 13 μ polyimide film.[17] About 10 cm^3 of hydrogen was condensed from a closed gas reservoir at atmospheric pressure. In the early runs of the experiment liquid helium flowing through a heat exchanger served as the refrigerator. Later we substituted a closed-cycle refrigerator[18] operating on helium gas. The target was situated in a 2-m-long field-free straight section of the synchrotron (Fig. 5) about 1 cm from the normal orbit toward the center of the synchrotron ring. A thin window on each side of the synchrotron vacuum chamber allowed for the exit of the pions and scattered electrons.

C. Beam Monitor

Because of multiple beam traversals and the cylindrical form of the target, knowledge of the number of incident electrons is not sufficient to measure a cross section. To do this we need to know $\langle N_e l \rangle$, the effective product of number of electrons and their traversal path length through the target. A convenient monitor of $\langle N_e l \rangle$ is the forward bremsstrahlung flux from the target. This was observed in a total absorption quantameter[19] outside the synchrotron ring directly downstream from the target (see Fig. 5). The total bremsstrahlung energy U absorbed by the quantameter is related to $\langle N_e l \rangle$ by

$$U = \eta \langle N_e l \rangle E / X_0 \quad (7)$$

for a target of uniform composition, with radiation length X_0. Ions made in the quantameter gas were collected and the current integrated. The calibration constant, $(5.06 \pm 0.15) \times 10^{15}$ GeV/coulomb, has been computed[19] from shower theory and checked by comparison with Faraday cup.[20] The efficiency factor η takes account of the finite solid angle of the quantameter, absorption along the bremsstrahlung beam line, and other less well understood effects. It was determined by the following indirect procedure: We observed elastic ep scattering at

[17] "Kapton," manufactured by E. I. DuPont de Nemours and Company.

[18] "340 LS Cryodyne," manufactured by Arthur D. Little, Inc. The principle of operation is described by W. E. Gifford [Progr. Cryog. **3**, 51 (1961)].

[19] R. R. Wilson, Nucl. Instr. **1**, 101 (1957).

[20] R. Gomez, J. Pine, and A. Silverman, Nucl. Instr. Methods **24**, 429 (1963).

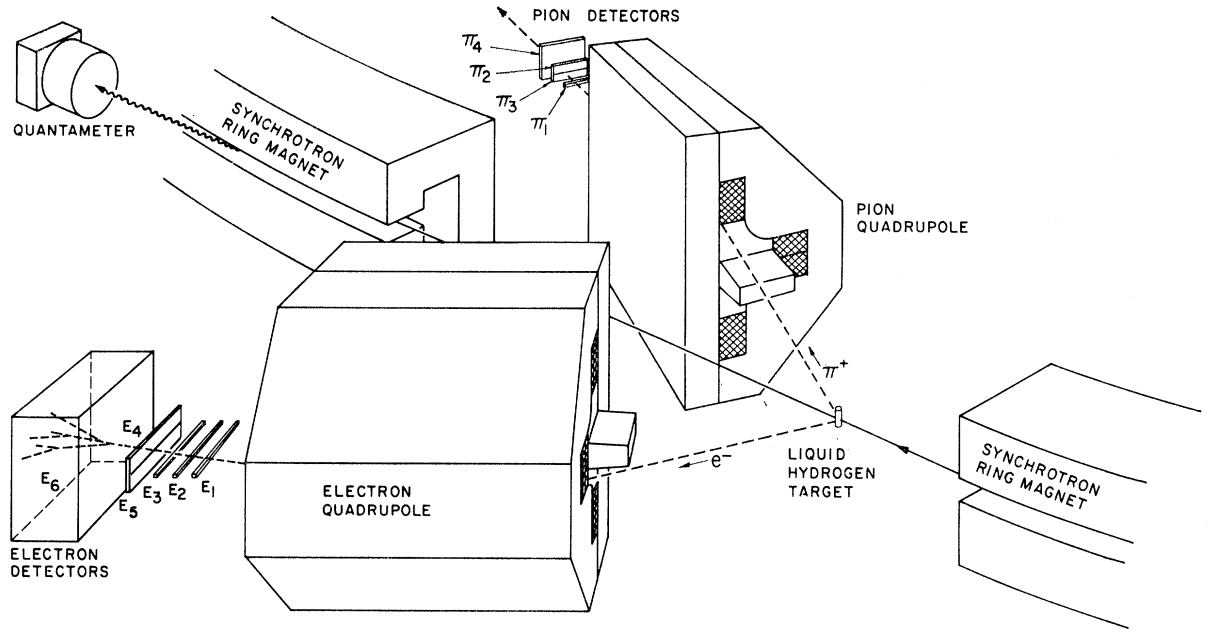

FIG. 5. Schematic view of the experimental layout.

some fixed energy and angle in a polyethylene target, and subtracted the background measured with a carbon target. From the net number of counts and the published cross section,[21] we computed the effective incident flux $\langle N_e l \rangle$, which we then substituted in (7) along with the observed quantameter response U in order to solve for η.

If the target is instead made of two different materials, hydrogen and walls, the energy going into the quantameter is

$$U=\eta(1+\delta)\langle N_e l_{\mathrm{H}}\rangle E/X_{\mathrm{H}}, \tag{8}$$

where δ is the bremsstrahlung intensity contributed by the walls relative to the bremsstrahlung from hydrogen; that is,

$$\delta=l_W X_{\mathrm{H}}/l_{\mathrm{H}} X_W. \tag{9}$$

It is not possible to determine δ simply by comparing the bremsstrahlung yield with target full and target empty because of the change in number of traversals. A crude estimate can be made from (9), the geometry of the target, and the spatial distribution of radiation damage on the polyimide walls. This gives $\delta=0.8\pm0.5$. A more accurate value was obtained by making an elastic ep scattering measurement in liquid hydrogen, then taking the observed yield and the known cross section[21] to compute the flux product $\langle N_e l_{\mathrm{H}}\rangle$, which was used in (8) along with the known U, η, E, and X_{H} to obtain δ. This gave $\delta=0.6\pm0.3$ for the range of incident energies used in this experiment.

It should be noted here that the bremsstrahlung monitor served only as a running tally of the incident beam flux. The absolute normalization of the measured electroproduction cross sections was based on measurements of the elastic cross section (see Sec. IV B for details).

D. Spectrometers

The momentum analysis of the electrons and pions was performed in the same way, using quadrupole spectrometers. A single quadrupole magnet, focusing in the vertical plane, forms a horizontal-line image of a point source. The image line intersects the quadrupole axis at right angles behind the magnet, at a distance which depends on the particle momentum. A long narrow scintillation detector placed at the image then defines the momentum, provided the median plane of the quadrupole is blocked (otherwise any particle can pass down the axis regardless of momentum).

Actually, each magnet was only half a quadrupole. A conventional quadrupole magnet of length 1.22 m and inscribed diameter 30.5 cm was split along a vertical plane through the axis. Each half was then closed with a 15-cm-thick slab of iron (see Fig. 5). The field pattern in each magnet half was then exactly the same as before the split. This enabled us to place the spectrometers at smaller angles with respect to the beam line than would have been possible with conventional quadrupoles. The minimum angles were 15° on the outside of the synchrotron ring, where we detected the electrons, and 20° on the inside.

The plug blocking the axis of each quadrupole was a tapered piece of lead about 5-cm high and 15-cm deep. It was mounted at the entrance to the magnet and

[21] We have assumed the Rosenbluth formula and the form factors $G_{Ep}=G_{Mp}/\mu_p=G_{Mn}/\mu_n=(1-k^2/0.71\ \mathrm{GeV}^2)^{-2}$, $G_{En}=0$. Evidence for this is discussed by M. Goitein, J. R. Dunning, and R. Wilson, Phys. Rev. Letters 18, 1019 (1967).

divided the aperture into two equal parts, one above and one below. Behind the lead plug was a 2.5-cm-high brass slab extending all the way through the magnet. The top and bottom aperture limits were defined inside the magnet by two brass strips.

Each magnet was mounted on a carriage attached to a pivot under the target. Target-to-magnet distances were typically 1 m. Angles were surveyed to $\pm 0.03°$ with respect to the 0° line established by observing the bremsstrahlung beam. The solid angle subtended at the target by each spectrometer was typically 3 to 5 msr, covering an angular range in the horizontal plane of 1° to 2° (determined by the length of the detectors).

The momentum resolution was determined by the vertical dimension h of the momentum-defining scintillator, according to the approximate relation $\Delta p/p \approx h/$ (9 cm) derived from ray-tracing computations. On the electron side three adjacent momentum channels spanned a momentum bite of 12%. On the pion side one momentum channel covered about 10%.

E. Detectors and Electronics

Scattered electrons were detected in the following array of counters: one of the three momentum-defining scintillators E_1, E_2, E_3, then one of two back-up scintillators, E_4 above the quadrupole axis and E_5 below, and finally a large lead-glass Čerenkov shower counter E_6. Pions were detected in the pion momentum-defining counter Π_1, then one of a pair of back-up scintillators Π_2, Π_3 like those on the electron side, and finally after passing through 6 to 19 mm of copper, another scintillator Π_4. Electron and pion detectors were mounted on the back of their respective quadrupoles (see Fig. 5).

A π^+ electroproduction event was defined as a sixfold coincidence (E_1 or E_2 or E_3) (E_4 or E_5)E_6 Π_1(Π_2 or Π_3)Π_4. Signals from the three electron momentum counters E_1, E_2, E_3, were mixed, and the detailed momentum information was not used in this experiment except as a consistency check. Four kinds of coincidences were recorded depending on whether E_4 or E_5 had a pulse and whether Π_2 or Π_3 had a pulse, thus defining which half of the quadrupole aperture was involved for each particle. For the up-down and down-up $e\pi$ coincidences the pion was detected close to the electron scattering plane, while for the up-up and down-down combinations the pions were slightly out of the electron scattering plane, by about 15° in the pion-nucleon center-of-mass frame.

The discriminator threshold on the lead-glass Čerenkov counter pulse was set high enough to ensure that a high-energy electron shower had been produced; all other thresholds were set below the pulse amplitude corresponding to the passage of a minimum ionizing particle. To improve the rejection of accidental coincidences, the sixfold $e\pi$ coincidence (about 20-nsec resolving time) triggered a time-to-pulse-height converter which displayed on a 100-channel analyzer the spectrum of time differences between the threefold electron coincidence and the threefold pion concidence. The result was always a true coincidence peak, 2.3 nsec fwhm (full width at half-maximum) superimposed on a uniform random background. The singles rates in all counters, and the pulse-height spectrum of the shower counter were monitored continuously, thus providing a sensitive check on the operation of the counters and electronics.

IV. MEASUREMENTS

A. Apertures

In order to fix all five independent variables on which the differential cross section can depend, it is sufficient to establish the incident energy E, the direction of the pion and of the scattered electron, and the momentum of either the pion or the electron. The other momentum is constrained by momentum and energy conservation, so its measurement is redundant. The redundancy is useful in suppressing background from other reactions, but it implies that the accepted momentum range should be defined by one of the two spectrometers and overmatched in the other. Since W and k^2 vary more slowly with pion momentum than with electron momentum, we chose to set the momentum bite with the pion spectrometer. The electron momentum resolution was made more than wide enough to accept the corresponding electrons. The cross section actually measured then was $d\sigma/dq d\omega_e d\omega_\pi$; it was converted to $d\sigma/dE' d\omega_e d\Omega_\pi$ by a Jacobian transformation.

Each time a spectrometer was moved its performance was checked by observing the yield of elastically scattered electrons as a function of the magnet current. A second lead-glass Čerenkov counter was placed behind the pion spectrometer and put in coincidence with the other counters in order to make this test on the pion spectrometer. A comparison of the peak electron rate with the rate predicted from known ep cross sections checked the spectrometer solid angle. This was also verified by occultation at the entrance to the quadrupole. A comparison of the rates for particles passing through the top and bottom halves of the aperture checked the vertical alignment. The magnet current at which the elastic peak was observed provided a momentum calibration point for the spectrometer. The shape of the elastic peak measured the momentum-resolution function. All these experimental checks agreed within the accuracy of the measurements with predictions based on ray-tracing computations, modified to account for multiple scattering in the air path and the vacuum chamber window.

One effect of multiple scattering in the air path is a random shift in the apparent momentum of the particle. This causes a net loss in counting rate if the momentum of the particle is already kinematically constrained, as it is both in the case of elastic scattering with a single spectrometer or in electroproduction measurements

using two spectrometers. The loss in the latter case is small, provided the momentum resolution of one spectrometer is sufficiently oversize. This was true for our experiment at the small electron scattering angles, but at the larger angles (implying lower electron momenta) the overmatch was not really enough. For these points the correction for loss due to multiple scattering was 10 to 50%. Since the statistical counting errors in the large-θ_e data were already quite large, the uncertainty in the multiple-scattering correction did not have a serious effect on the accuracy of those measurements.

B. Rates

Electroproduction measurements were made at three values of momentum transfer $-k^2=1$, 3, and 6 F^{-2}, at three values of W in the vicinity of the $N^*(1230)$ resonance $W=1175$, 1200, and 1300 MeV, and for polarization values ranging from $\epsilon=0.44$ to $\epsilon=0.92$ (see Table I). Incident energies E ranged from 540 to 1750 MeV, electron lab angles θ_e from 15° to 60°, and pion lab angles (with respect to the incident electron direction) from 22° to 43°.

For each π^+ electroproduction point, the following measurements were made, both with hydrogen in the target and with the target empty.

(1) The elastic electron scattering rate R_e (counts per unit energy U deposited in the quantameter). This was measured using the electron spectrometer only, at the same incident energy and scattering angle to provide cross-section normalization. The measurement was repeated many times, interspersed with the $e\pi$ measurements in order to monitor any drifts in the apparatus.

(2) The $e\pi^+$ coincidence rate $R_{e\pi}$. The rate ranged from about 10 counts/h at small electron angles to about 1 count/h at the largest angles. The statistical accuracy after subtraction of accidental coincidences was typically 8% in the former case and 20% in the latter.

(3) The ep coincidence rate R_{ep} from π^0 electroproduction at $\Theta_\pi=180°$ and the same W, k^2, and ϵ. Since this rate was usually an order of magnitude higher than the $e\pi^+$ rate (mainly because of a more favorable Jacobian factor), it served as a convenient check on the equipment. However, since only a small fraction of the running time was invested in this, the statistical accuracy obtained was somewhat poorer than in the $e\pi^+$ data.

Since the pion counters were equally sensitive to pions and photons, the change from $e\pi^+$ coincidences to ep coincidences was made by resetting just the current in the pion magnet and the delay cable length. The time-of-flight difference between pions and protons was typically 10 nsec.

In elastic scattering the electron momentum at a given angle is constrained by two-body kinematics. In electroproduction the detection of the pion at fixed momentum imposes a completely analogous constraint on the electron momentum. The ratio of net rates then depends only on the ratio of differential cross sections and on the pion aperture $\Delta q\Delta\omega_\pi$.

Since the average number of traversals of the beam particles through the target changed when the target was emptied, the empty-target rates could not be subtracted directly from the full-target rates to get the net hydrogen rates. It is easy to show from (7), (8), and (9) that the empty-target rate must be multiplied by $\delta(1+\delta)^{-1}$ before subtracting. The π^+ electroproduction differential cross section is therefore given in terms of the measured rates and the known elastic cross section[21] by

$$\frac{d\sigma}{dqd\omega_e d\omega_\pi}=\frac{d\sigma^e/d\omega_e}{\Delta q\Delta\omega_\pi}\frac{R_{e\pi}{}^{\text{full}}}{R_e{}^{\text{full}}}\frac{1-\delta(1+\delta)^{-1}r_{e\pi}}{1-\delta(1+\delta)^{-1}r_e}, \quad (10)$$

where $r_{e\pi}=R_{e\pi}{}^{\text{empty}}/R_{e\pi}{}^{\text{full}}$ and $r_e=R_e{}^{\text{empty}}/R_e{}^{\text{full}}$. The same formula holds for the ep coincidence measurements. The empty-target relative rates were typically $r_e\approx0.3$, $r_{e\pi}<0.1$, and $r_{ep}\approx0.3$. Note that although δ is only poorly known (see Sec. IIIC,) the uncertainty in the ratio

$$\frac{1-\delta(1+\delta)^{-1}r_{e\pi}}{1-\delta(1+\delta)^{-1}r_e}$$

is only 4%, and the corresponding ratio in the ep case is uncertain to less than 2%. Notice also that several other possible sources of error have been eliminated by normalizing the electroproduction data to elastic data: the quantameter efficiency η and the electron-spectrometer solid angle $\Delta\omega_e$, for example. The ratio of electroproduction and elastic cross sections is very much less sensitive to errors in setting θ_e and E than are the cross sections themselves.

The uniform background of accidental coincidences (<10%) in the time-of-flight spectrum was subtracted from the rates in the coincidence peak. The $e\pi^+$ rates were corrected for decay of the pion in flight (about 20%), and both the $e\pi^+$ and ep data were corrected by about 5% for nuclear absorption. The radiative corrections (see Appendix II) for electroproduction observed with electron-pion coincidences, and for elastic scattering with only the electron observed, turn out to be very nearly equal, leaving a net correction of $0\pm2\%$ in the ratio. Radiation of real photons by the incident and scattered electron in the target had a negligible effect. The net estimated error arising from uncertainties in Δq, $\Delta\omega_\pi$, and the corrections for decay, absorption, and radiation was about 7%.

C. Cross Sections

Each measured π^+ or π^0 electroproduction cross section actually consisted of two measurements. One presented pions produced in or very near the electron scattering plane, and corresponded to the spectrometer

TABLE I. Measured π^+ virtual photoproduction cross sections for $\Theta_\pi=0$. Also tabulated are the best-fit pion form factors and our estimate of the error in the theoretical predictions of Ref. 24. The errors listed for F_π are experimental only; the theoretical error is shown in Fig. 9.

$-k^2$ (F^{-2})	$-k^2$ (GeV/c)^2	W (MeV)	ϵ	$d\sigma_v/d\Omega_\pi$ (μb/sr)	$F_\pi(k^2)$	Theor. error in $d\sigma_v/d\Omega_\pi$
1.0	0.039	1175	0.85	10.9 ± 1.6	$0.79_{-0.13}{}^{+0.11}$	15%
3.0	0.117	1175	0.92	12.4 ± 1.1	$0.87_{-0.06}{}^{+0.05}$	8%
3.0	0.117	1175	0.44	1.8 ± 0.8[a]		
3.0	0.117	1200	0.92	13.8 ± 1.1	$0.79_{-0.05}{}^{+0.04}$	7%
3.0	0.117	1200	0.76	$12.8_{-1.0}{}^{+2.6}$	$0.84_{-0.06}{}^{+0.13}$	7%
3.0	0.117	1200	0.45	9.0 ± 2.2	$0.82_{-0.25}{}^{+0.20}$	8%
3.0	0.117	1300	0.89	23.1 ± 1.8	$0.91_{-0.10}{}^{+0.09}$	15%
3.0	0.117	1300	0.68	17.1 ± 1.7	$0.70_{-0.16}{}^{+0.11}$	19%
6.0	0.234	1175	0.92	5.9 ± 0.7	$0.57_{-0.07}{}^{+0.06}$	9%
6.0	0.234	1175	0.50	3.3 ± 2.6[a]		

[a] The errors were too large in these cases to allow a form factor determination.

apertures up-down and down-up (see Sec. III D); the other represented pions slightly out of the plane, corresponding to the up-up and down-down combinations. For the π^+ data the two rates were not significantly different, but for π^0 they were. Each of the partial apertures also spanned a range in the kinematic variables comparable to the interval between the two apertures; typically, for π^+, $\Delta W=2$ MeV (20 MeV for π^0) and $\Delta\Theta_\pi=15°$ (30° for π^0).

In order simplify the interpretation of the data, we have shifted and combined each pair of measurements so that it refers to rounded values of k^2 and W and to $\Theta_\pi=0$ (or 180° for π^0). The shifts in the measured cross-section values were obtained from a phenomenological model of electroproduction (the propagator model described in the next section of this paper). The absolute values of the theoretical cross sections were not used, only the predicted rates of change with respect to k^2, W, and Θ_π. The net change in the measured values was 15% at the most, and the error thus introduced was estimated to be about 2%.

The shifted experimental cross sections $d\sigma/dE'd\omega_e d\Omega_\pi$ were reduced to virtual photoproduction cross sections $d\sigma_v/d\Omega_\pi$ [see Eq. (4)] by dividing out the electrodynamics factor, which contains most of the rapid variation with E and θ_e. These are then listed in Tables I and II with the corresponding estimated experimental errors. The tabulated cross sections should apply to the given rounded values of k^2 and W and for $\Theta_\pi=0°$ (or 180°).

TABLE II. Measured π^0 virtual photoproduction cross section for $\Theta_\pi=180°$. Also listed are the theoretical predictions of Ref. 24.

$-k^2$ (F^{-2})	$-k^2$ (GeV/c)^2	W (MeV)	ϵ	$d\sigma_v/d\Omega$ (expt.) (μb/sr)	$d\sigma_v/d\Omega_\pi$ (th.) (μb/sr)
1.0	0.039	1175	0.85	9.4 ± 1.8	10.0
3.0	0.117	1175	0.92	8.6 ± 0.9	8.6
3.0	0.117	1175	0.44	0.6 ± 0.3	8.3
3.0	0.117	1200	0.92	8.7 ± 0.9	10.8
3.0	0.117	1200	0.76	$10.3_{-0.9}{}^{+1.8}$	10.6
3.0	0.117	1200	0.45	5.1 ± 1.8	10.2
3.0	0.117	1300	0.89	1.8 ± 0.3	4.9
3.0	0.117	1300	0.68	1.7 ± 0.2	4.4
6.0	0.234	1175	0.92	2.8 ± 0.5	5.6
6.0	0.234	1175	0.50	1.0 ± 0.5	5.4

V. INTERPRETATION

A. Qualitative Features

We have plotted some of the π^+ electroproduction data in Figs. 6, 7, and 8 to show how $d\sigma_v/d\Omega_\pi$ depends on W, k^2, and ϵ. Figure 6 shows the variation with W, keeping the other parameters fixed. Just as in forward π^+ photoproduction the rise in cross section is due to the $N^*(1230)$ resonance; the peak is shifted to higher W by the interference with the nonresonant background. In Fig. 7 we see the momentum-transfer dependence. The initial increase is probably caused by the rise in the longitudinal contribution, which vanishes at $k^2=0$; the eventual decrease follows the decrease of the nucleon and pion form factors. Figure 8 shows the dependence

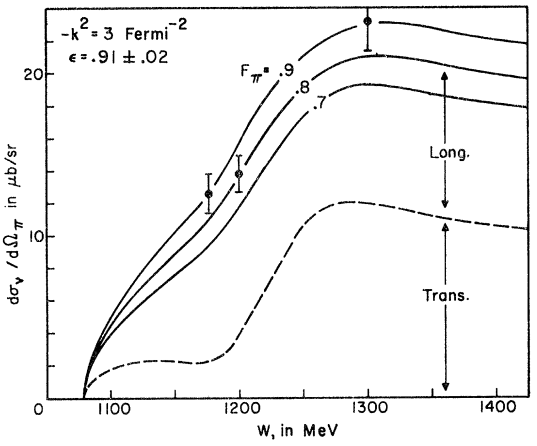

FIG. 6. The π^+ virtual photoproduction cross section as a function of W for $k^2=-3$ F^{-2}, $\epsilon=0.89$, and $\Theta_\pi=0$. Data are from this experiment. Theoretical curves for various values of F_π are computed from Ref. 24.

of the virtual photoproduction cross section on the polarization parameter ϵ at fixed W, k^2, and $\Theta_\pi=0$. Quantum electrodynamics and the assumption of single-photon exchange lead us to expect a form $d\sigma_v/d\Omega_\pi=A+\epsilon B$ [Eq. (6)], a straight-line plot with an intercept A equal to the transverse contribution and a slope B equal to the longitudinal contribution. The data points in Fig. 8 are consistent with a straight line and indicate an appreciable slope, clear evidence of the presence of longitudinal photons.

In Sec. II we have shown that at $\Theta_\pi=0$ the entire dependence of $d\sigma_v/d\Omega_\pi$ on the pion form factor comes in the longitudinal term. It would seem reasonable then to fit a straight line to the polarization dependence (Fig. 8) and eliminate the transverse background to obtain a cleaner determination of F_π. An accurate value for the slope, however, requires accurate data widely spaced in ϵ. In practice it is extremely difficult to obtain any accuracy for small ϵ because small ϵ implies large scat-

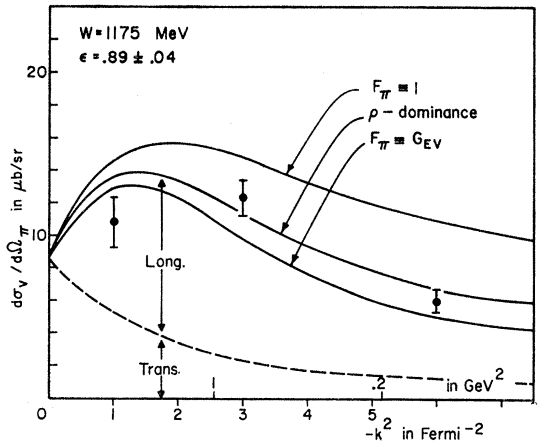

FIG. 7. The π^+ virtual photoproduction cross section as a function of the momentum transfer k^2 for $W=1175$ MeV, $\epsilon=0.91$, and $\Theta_\pi=0$. Data are from this experiment. Theoretical curves for various pion form factor models are computed from Ref. 24. The ρ-dominance model refers to Eq. (13).

tering angle θ_e (see Fig. 3), which means very low counting rates. The electrodynamics factor in (4) drops by an order of magnitude from $\theta_e=15°$ to 45° at fixed k^2 and W. Therefore, in order to interpret these data in terms of the pion form factor we require a theoretical model for the full transverse-plus-longitudinal cross section.

B. Theory of Electroproduction

Most recent theoretical treatments of photoproduction and electroproduction have been based on dispersion relations, first applied to these phenomena by Chew, Goldberger, Low, and Nambu[22] and Fubini, Nambu, and Wataghin.[23] In this type of theory the cross section is expressed in terms of the kinematic variables, the masses, the coupling constants e and f, the $T=\frac{3}{2}$, $J=\frac{3}{2}^+$ resonant πN phase shift, and in the case of electroproduction, the nucleon and pion form factors. The most recent numerically explicit dispersion calculation of the photoproduction and electroproduction differential cross sections available in the published literature at the date of this writing is that of Zagury.[24] It is fully relativistic, includes recoil corrections, is insensitive to cutoff, and reduces to the CGLN[22] and FNW[23] theories in the static limit. Other dispersion calculations[23,25] are qualitatively similar and predict cross sections which differ by less than 10% over the range of kinematic variables covered in this experiment.

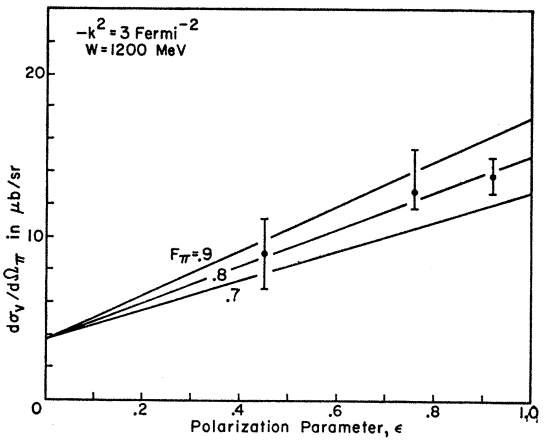

FIG. 8. The π^+ virtual photoproduction cross section as a function of the polarization parameter ϵ for $W=1200$ MeV, $k^2=-3$ F^{-2}, and $\Theta_\pi=0$. Data are from this experiment. Theoretical curves for various values of F_π are computed from Ref. 24. The intercept at $\epsilon=0$ is the transverse contribution; the part proportional to ϵ is the longitudinal.

A simpler phenomenological treatment of photoproduction and electroproduction is offered by the propagator model,[26] which replaces the resonance-dominated dispersion integrals by Feynman amplitudes corresponding to an $N^*(1230)$ intermediate state [Fig. 1(d)], viewing the N^* as an elementary particle with complex mass and the appropriate quantum numbers. This approach introduces three undetermined functions of k^2 to specifiy the γNN^* couplings. These can be fit to experiment but the conclusions depend on which data are emphasized; so we view this as somewhat unreliable, especially for $k^2\neq 0$. Furthermore, there seems to be some controversy[27] among the experts as to the proper form for the $J=\frac{3}{2}^+$ propagator. The dispersion theoretic result may be just as unreliable but at least it is explicit, and there is no chance of our biasing the interpretation of our data by making prejudiced choices of parameters in the theory. The propagator model with reasonable choices of parameters[28] leads to the same cross-section values as the dispersion calculation within 10%, and the over-all agreement with the available data is about the same.

We use the results of Zagury's calculation[24] in the analysis of our data. That is, the theoretical cross section $d\sigma_v/d\Omega_\pi$ is evaluated for each of the data points

[22] G. F. Chew, M. L. Goldberger, F. E. Low, and Y. Nambu, Phys. Rev. **106**, 1345 (1957).

[23] S. Fubini, Y. Nambu, and V. Wataghin, Phys. Rev. **111**, 329 (1958).

[24] N. Zagury, Phys. Rev. **145**, 1112 (1966). Differential cross sections corresponding to our data points were not published in Zagury's paper. He has very kindly computed them for us, however.

[25] S. L. Adler, in Proceedings of the International Conference on Weak Interactions, Argonne Report No. ANL-7130, 1965, p. 285 (unpublished); and S. L. Adler (private communication).

[26] This is often referred to as the "isobar model"; but since this term means different things to different people, we avoid confusion by not using it. The model was first used by S. Minami, T. Nakano, K. Nishijima, H. Okonogi, and E. Yamada, Progr. Theoret. Phys. (Kyoto) **8**, 531 (1952). Its relation to the dispersion theory has been discussed by D. Amati and S. Fubini, Ann. Rev. Nucl. Sci. **12**, 359 (1962).

[27] E. Abers and C. Zemach, Phys. Rev. **131**, 2305 (1963); G. Höhler and W. Schmidt, Ann. Phys. (N. Y.) **28**, 34 (1964); G. Höhler, in *Proceedings of the International Symposium on Electron and Photon Interactions at High Energies, Hamburg, 1965*, edited by G. Höhler *et al.* (Deutsche Physikalische Gesellschaft, Hamburg, 1965), Vol. I, p. 55.

[28] J. P. Loubaton, Nuovo Cimento **39**, 591 (1965).

(Table I), using the known nucleon form factors[21] and leaving the pion form factor F_π as the only free parameter. For each data point we then determine the $F_\pi(k^2)$ which gives agreement between theory and experiment, and the corresponding limits on F_π which give one standard deviation discrepancy (see Table I). The limits on F_π listed in Table I refer only to the experimental errors and do not take account of possible errors in the theory.

C. Reliability of the Theory

To estimate the possible limits of accuracy of Zagury's calculation we first check the theory against the available experimental data:

(1) π^0 photoproduction. Plots of the theoretical differential cross sections compared with the experimental data are given in Zagury's paper.[24] The agreement is fair ($\pm 20\%$) where the cross section is large, but gets worse at extreme angles and in the tails of the resonance.

(2) π^0 electroproduction. There are four experiments: (a) a single measurement by Perez *et al.*[4] at $-k^2=1.3$ F^{-2}, $W=1210$ MeV, $\epsilon=0.41$, $\Theta_\pi=125°$, $\phi=180°$; (b) another one by Kikuchi *et al.*[29] at $-k^2=2.3$ F^{-2}, $W=1190$ MeV, $\epsilon=0.56$, $\Theta_\pi=65°\pm 40°$, $\phi=205°\pm 25°$; (c) four measurements by Ash *et al.*[30] at $-k^2=1$ to 8 F^{-2}, $W=1230$ MeV, $\epsilon=0.8$ to 0.9, $\Theta_\pi=90°$, $\phi=180°$; and (d) a number of measurements at $\Theta_\pi=180°$ made in the course of this experiment (see Table II). The results of both the Perez and Kikuchi experiments fall short of the theory by about a factor of two; however, in both cases the experimental error was about 50%. The later measurements of Ash *et al.* (about 15% accuracy), agree with the theoretical predictions or exceed them by less than 20%. Moveover, these data extrapolate at $k^2=0$ to the measured 90° resonance photoproduction, which also exceeds the theoretical result by about the same factor. The agreement between the 180° data and the theory (Table II) is only fair to poor. The discrepancies however, are very similar to those observed for 180° π^0 photoproduction.

(3) π^+ photoproduction. Figures 7 and 8 of Zagury's paper[24] show a comparison of the predicted angular distribution and the experimental data. The agreement is generally better than in the π^0 case. It is important for our present purposes to note the comparison in the forward direction (Fig. 9 of this paper). Here the discrepancy is less than 10% around $W=1200$ MeV, but to either side of the resonance, the experimental cross sections fall below the theory by as much as 25%.

(4) π^+ electroproduction. Except for the present experiment, the only source of π^+ electroproduction data is the work of Akerlof *et al.*[5] Because of the rather large experimental errors, the data provide only qualitative support for the thoery.

(5) Inelastic electron scattering. In Figs. 13 and 14 of his paper[24] Zagury compares his theoretical results (the lower of the pair of curves) with the data of Hand.[3] In the region of the resonance the experimental cross sections are 0 to 15% above the theoretical curve. The agreement gets worse above the resonance.

We consider separately the transverse and longitudinal parts A and B of the virtual photoproduction cross section. First of all, it is clear that no existing data tell us anything about B, the longitudinal contribution. It is absent in photoproduction, and its contribution to π^0 electroproduction turns out to be very small in all models. Its presence in the inelastic electron spectra has not been detected. And since only B has any sensitivity to the pion form factor, none of the above comparisons are affected by the choice of F_π. The theoretical predictions have been checked for the effect of a variation of 0.05 in the assumed value of G_{En}, which produces a variation of the order of 15% in A and 1% in B, and for the effect (5%) of including a ρ-exchange diagram. The π^0 photoproduction and electroproduction data seem to indicate that the discrepancies between theory and experiment are not strongly dependent on k^2. If the same is true of the π^+ production, we can conclude from the comparison of the theory with the π^+ photoproduction (Fig. 9) that $A(W,k^2,0°)$, as given by Zagury, is probably correct to about 15% or better at $W=1200$ MeV, and may be wrong by 25% at $W=1175$ and 1300 MeV.[31] We do not try to adjust the theory to make it agree, but instead we can use the discrepancy as a measure of the theoretical uncertainty. In the range of kinematic variables covered by this experiment the longitudinal amplitude is relatively simple and noncontroversial. It is given by the Born amplitudes Fig. 1(a), (b), (c) with very little rescattering correction Fig. 1(d). Since the theoretical error in B is likely to be much smaller than the error in A, we rather arbitrarily assume it to be 5%.

D. Form Factor Results

The determination of the pion form factor from our data is certainly not without model-dependent uncer-

[29] R. Kikuchi, K. Baba, S. Kaneko, K. Huke, Y. Kobayashi, and T. Yamakawa, Nuovo Cimento **43**, 1178 (1966).

[30] W. W. Ash, K. Berkelman, C. A. Lichtenstein, A. Ramanauskas, and R. H. Siemann, Phys. Letters **24B**, 165 (1967).

[31] It is probably true that the dispersion calculation is more reliable for π^+ production than for π^0. The nonresonant contribution to π^0 production is sensitive to errors in the theory because it comes from two partially canceling diagrams [Figs. 1(a) and (b)], only one of which is important in π^+ production. In its usual formulation (Ref. 28) the propagator model inserts an adjustable s-wave correction affecting mainly the π^0 production. Without it the π^0 cross section peaks strongly at 180° and is ten times too large at $W=1300$ MeV. Its effect on the π^+ is only a smooth 10–15% decrease in the cross section. In the dispersion theory these corrections are given automatically by the s-wave projections of the resonance integral. For the π^0 they are large, but not as large as in the phenomenological fit; hence the dispersion result does not match the π^0 experimental data very well, especially at 180°. In the π^+ production, however, these terms are small and close to the best fits, so there is more hope here for the validity of the dispersion result.

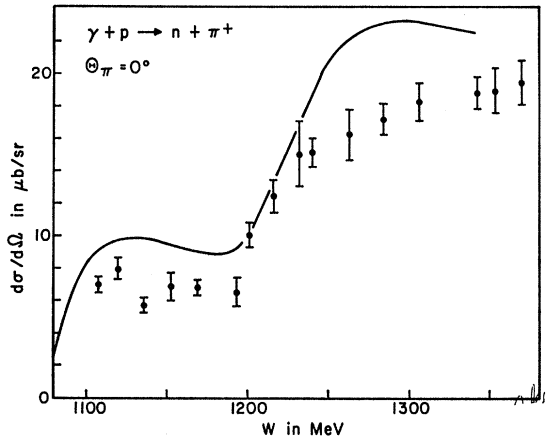

FIG. 9. The ordinary π^+ photoproduction cross section at 0° as a function of W. Data are from the compilation of J. T. Beale, S. D. Eklund, and R. L. Walker, CTSL-42 (unpublished). The theoretical curve is taken from Ref. 24.

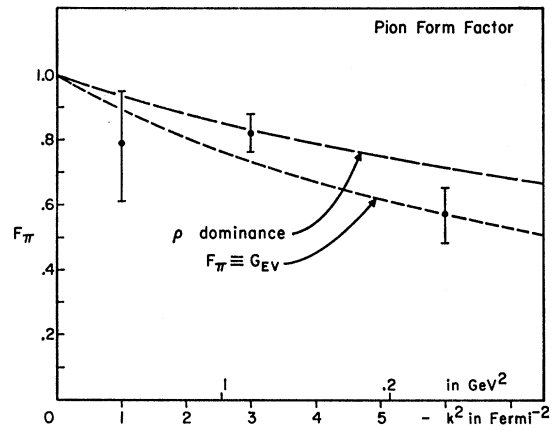

FIG. 10. The pion charge form factor as a function of momentum transfer. Data are obtained by fitting the measured cross sections (Table I) to theory (Ref. 24). Error limits include experimental error and an estimate of the reliability of the theory, combined quadratically. The ρ-dominance model is given by Eq. (13).

tainties. We nevertheless make the attempt with the following justifications. First, the measured cross sections are really very sensitive to F_π. The longitudinal cross section makes up 50–80% of the total and is dominated by a term proportional to F_π^2. So the uncertainties in the transverse part do not prevent at least a rough determination of F_π. Secondly, the values of F_π derived from data taken at the same k^2 but different W and ϵ (see Figs. 6 and 8) are remarkably consistent. This is actually a rather severe test of the theory, since the measured cross sections can vary rapidly with W and ϵ. Thirdly, this analysis of our data is meant to be only tentative. We hope and trust it will inspire others to make further refinements in the theory of electroproduction and improve the reliability of the determination of the pion form factor.

Our assumptions about the accuracy of the Zagury calculation lead to the theoretical error limits in Table I. They tend to be somewhat smaller than the corresponding experimental errors. Theoretical errors are not independent, but are very likely to be strongly correlated from one data point to another. Their effect does not decrease when we average the six measurements of $F_\pi(-3\ \mathrm{F}^{-2})$. Figure 10 shows the weighted averages for F_π. The error limits were obtained by combining theoretical and experimental errors quadratically.

VI. DISCUSSION

Before discussing the significance of our measurements of the pion form factor we must establish the validity of a form factor measured on virtual pions. Is it the same as the form factor one would obtain by scattering electrons off free pions? The target pions in this experiment were off the mass shell by an amount $(p_\mu - p_\mu')^2 - \mu^2$ ranging from $-1.5\mu^2$ to $-5.7\mu^2$. The resulting effect on the pion pole amplitude (form factor *and* propagator) may, however, turn out to be quite small, since the generalized Ward identity[32] can be used to show, first, that the correction must vanish in the low k^2 limit, and second, that the correction vanishes for all k^2 provided that the pion charge structure can be accounted for by diagrams in which a single particle (a vector meson, say) couples the photon to the pion.[33]

Electroproduction is not the only reaction involving the pion charge form factor. Pion-electron elastic scattering[34] and the difference between π^+-helium and π^--helium elastic scattering[35] have been used to measure the form factor at very small values of momentum transfer ($-k^2 = 0.3$ F^{-2} and 0.6 F^{-2}, respectively), or equivalently, the pion charge radius.[36] So far, only upper limits on the root-mean-square radius have been obtained: $r_\pi < 3$ F from πe scattering and $r_\pi < 1.5$ F from $\pi\alpha$ scattering. Both are consistent with the electroproduction result.

The Dalitz decay of the neutral pion $\pi^0 \to e^+ + e^- + \gamma$ involves a $\pi^0\gamma\gamma$ vertex in which one of the photons is virtual. The spectrum of e^+e^- pairs[37] depends on the vertex form factor $f_{\pi\gamma\gamma}(k_\gamma^2)$. Although this electromagnetic form factor is often referred to as "the pion form factor," it has no obvious relation with the $\pi\pi\gamma$ form factor F_π, and any "radius" derived from $f_{\pi\gamma\gamma}$ is not the radius of the pion charge distribution.

Since the suggestion by Frazer and Fulco,[38] the

[32] F. E. Low, Phys. Rev. **110**, 974 (1958).
[33] D. R. Yennie (private communication).
[34] J. Allen, G. Ekspong, P. Sällstrom, and K. Fischer, Nuovo Cimento **32**, 1114 (1964); D. Cassel, M. Barton, R. Crittenden, F. Fitch, and L. Leipuner (unpublished).
[35] M. M. Sternheim and R. Hofstadter, Nuovo Cimento **38**, 1854 (1966); M. E. Nordberg and K. F. Kinsey, Phys. Letters **20**, 692 (1966); G. B. West, Phys. Rev. (unpublished).
[36] The root-mean-square radius is defined in terms of the initial slope of the form factor: $r = (6dF/dk^2)^{1/2}$ at $k^2 = 0$.
[37] P. Némethy, S. Devons, E. DiCapua, C. Nissim-Sabat, and A. Lanzara, Bull. Am. Phys. Soc. **12**, 567 (1967); N. Samios, Phys. Rev. **121**, 275 (1961).
[38] W. R. Frazer and J. R. Fulco, Phys. Rev. Letters **2**, 365 (1959).

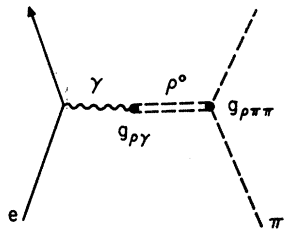

FIG. 11. Diagram representing electron-pion scattering in the ρ-dominance model.

vector-meson exchange model has been the most popular explanation of the momentum-transfer dependence of the nucleon form factors, although the quantitative agreement with the data is not very good.[10] Let us apply this model to the pion. Consider first the elastic scattering of an electron and a charged pion (Fig. 11). In the t channel, e^+e^- annihilation into π pairs, we expect the amplitude to be dominated by any two-pion resonant state which has the quantum numbers of the photon. This means $J^P=1^-$ and odd under C. Two bosons in an antisymmetric spatial state ($l=1$) must be in an antisymmetric charge state, hence, $T=1$. The G parity, given by $G=C(-1)^T$, is then even. We therefore expect $e\pi$ scattering to be dominated by the exchange of $T=1$, $J^{PG}=1^{-+}$ meson states. The only known $T=1$ vector meson is the $\rho(760)$.

Ignoring the effect of the width of the ρ mass we can write

$$F_\pi(k^2)=\frac{g_{\rho\gamma}g_{\rho\pi\pi}}{m_\rho{}^2-k^2}, \tag{11}$$

where the g's refer to coupling constants (Fig. 11). We can make a consistency check on (11) using an argument due to Sakurai.[39] We evaluate (11) at $k^2=0$, noting that $F_\pi(0)=1$:

$$1=(g_{\rho\gamma}/m_\rho{}^2)g_{\rho\pi\pi}. \tag{12}$$

The constant $g_{\rho\pi\pi}$ is known from the 2π decay rate of the ρ^0:

$$\Gamma_{\rho\pi\pi}=\frac{2}{3}\frac{g_{\rho\pi\pi}{}^2}{4\pi}\frac{(\frac{1}{4}m_\rho{}^2-\mu^2)^{3/2}}{m_\rho{}^2}$$

$$=177\pm10\text{ MeV}.^{40}$$

This gives $g_{\rho\pi\pi}=5.37\pm0.25$. The other constant $g_{\rho\gamma}$ is known from the lepton pair decay rate of the ρ:

$$\Gamma_{\rho ll}=\tfrac{4}{3}\pi\alpha^2(g_{\rho\gamma}/m_\rho{}^2)^2(m_\rho{}^2-4m^2)^{1/2},$$

$$=6.1\pm1.0\text{ keV for }\rho^0\to e^+e^-,\text{ (Ref. 41)}$$

$$=5.9\pm1.3\text{ keV for }\rho^0\to\mu^+\mu^-.\text{ (Ref. 42)}$$

Taken together, the two measurements yield $g_{\rho\gamma}/m_\rho{}^2=0.19\pm0.01$. The right-hand side of (12) is then equal to 1.01 ± 0.08. That is, the ρ pole (Fig. 11) accounts for practically all of the pion charge.

The mass spectrum of μ pairs produced by pions on nuclei[43] is further evidence in favor of the ρ-pole dominance of the pion form factor. Provided the reaction proceeds through the one-pion-exchange pole,[44] the μ-pair spectrum is proportional to the pion form factor for timelike photons. Only the ρ peak is seen.

The fact that the vector-meson model, using the known $T=0$ and $T=1$ vector mesons, does not correctly represent the nucleon form factor behavior certainly tends to weaken our argument. Many suggestions have been made[10] to account for this. In some theories one would expect F_π to disagree with the simple pole prediction in the same way as the nucleon form factors do. In others, however, one would expect F_π to deviate from the ρ-pole model much less than do the nucleon form factors. Still others make no definite prediction. Although the nucleon data are very precise, they have not been able to resolve the various possibilities. Perhaps eventually we can narrow the range of possible models using data on the pion form factor.

If the simple ρ-exchange model is correct, we expect

$$F_\pi(k)=(1-k^2/m_\rho{}^2)^{-1}. \tag{13}$$

This is compared with our data in Fig. 10. It fits, with $\chi^2=4.5$. With the present accuracy, however, it is not possible to distinguish between the ρ-pole model and a behavior like the nucleon form factors, although the latter is slightly favored; $F_\pi\equiv G_{Ep}$ fits with a χ^2 of 2.2. If we fit[45] the data to (13) with a variable mass m, the best fit is obtained for $m=600\pm80$ MeV. This implies a root-mean-square pion charge radius of $r_\pi=(\sqrt{6})/m=0.80\pm0.10$ F.

ACKNOWLEDGMENTS

We are grateful to N. Zagury for providing us with numerical predictions based on his dispersion model of electroproduction, to D. R. Yennie for clarifying the effects of radiation and gauge invariance, to S. L. Adler and C. Mistretta for useful conversations, and to M. S. Livingston for the loan of a CEA quadrupole magnet.

[39] J. J. Sakurai, Phys. Rev. Letters **17**, 1021 (1966). Our $g_{\rho\pi\pi}$ is Sakurai's f_ρ.

[40] Weighted average of all experiments: A. H. Rosenfeld, A. Barbaro-Galtieri, W. J. Podolsky, L. R. Price, P. Soding, C. G. Wohl, M. Roos, and W. J. Willis, Rev. Mod, Phys. **39**, 1 (1967).

[41] From a mean of two measurements: M. N. Khachaturyan *et al.*, Phys. Letters **24B**, 349 (1967); C. C. Ting (private communication).

[42] From a mean of two measurements: J. K. dePagter *et al.*, Phys. Rev. Letters **16**, 35 (1966), (see also Ref. 10); and Ref. 44.

[43] A. Wehmann, E. Engels, L. N. Hand, C. M. Hoffman, P. G. Innocenti, R. Wilson, W. A. Blanpied, D. J. Drickey, and D. G. Stairs, Phys. Rev. Letters **17**, 1113 (1966).

[44] A. Wehmann, E. Engels, C. M. Hoffman, P. G. Innocenti, R. Wilson, W. A. Blanpied, D. J. Drickey, L. N. Hand, and D. G. Stairs, Phys. Rev. Letters **18**, 929 (1967).

[45] Other fits: ρ pole plus core, $F_\pi=a(1-k^2/m_\rho{}^2)^{-1}+1-a$ with $a=1.3\pm0.2$; dipole fit, $F_\pi=(1-k^2/m^2)^{-2}$ with $m^2=0.62\pm0.16$ GeV^2.

APPENDIX I. CONNECTION BETWEEN ELECTROPRODUCTION AND PHOTOPRODUCTION

A. Photoproduction

The photoproduction differential cross section in the center-of-mass system is given by[46]

$$\frac{d\sigma}{d\Omega_\pi}=\frac{1}{4(2\pi)^2}\frac{M^2Q}{W^2K}\frac{1}{4}\sum|\langle\pi N'|\epsilon_\mu J_\mu|N\rangle|^2,$$

where $K=|\mathbf{K}|$, ϵ_μ is the photon polarization vector, and J_μ is the hadron current operator. It is convenient to sum over spin and polarization before contracting the four-vectors:

$$\frac{d\sigma}{d\Omega_\pi}=\frac{1}{4(2\pi)^2}\frac{M^2Q}{W^2K}[\tfrac{1}{2}\sum\epsilon_\mu\epsilon_\nu^*]\times[\tfrac{1}{2}\sum\langle\pi N'|J_\mu|N\rangle\langle\pi N'|J_\nu|N\rangle^*].$$

The first bracket is by definition the polarization density matrix $e_{\mu\nu}$ of the photon beam. Abbreviating the second bracket by $T_{\mu\nu}$, we write

$$\frac{d\sigma}{d\Omega_\pi}=\frac{1}{4(2\pi)^2}\frac{M^2Q}{W^2K}e_{\mu\nu}T_{\mu\nu}. \tag{A1}$$

If we have an unpolarized transverse photon beam propagating along the z direction, then $e_{xx}=e_{yy}=\frac{1}{2}$ with all the other matrix elements zero:

$$\frac{d\sigma}{d\Omega_\pi}=\frac{1}{4(2\pi)^2}\frac{M^2Q}{W^2K}\frac{T_{xx}+T_{yy}}{2}. \tag{A2}$$

If the photon beam is partially linearly polarized, so that $e_{xx}=\frac{1}{2}(1+\epsilon)$ and $e_{yy}=\frac{1}{2}(1-\epsilon)$, we have

$$\frac{d\sigma}{d\Omega_\pi}=\frac{1}{4(2\pi)^2}\frac{M^2Q}{W^2K}\left[\frac{T_{xx}+T_{yy}}{2}+\epsilon\frac{T_{xx}-T_{yy}}{2}\right]. \tag{A3}$$

B. Electroproduction

Assuming single-photon exchange, the electroproduction cross section differential in the lab-scattered energy, lab-electron solid angle, and pion solid angle in the center-of-mass frame of the final pion plus nucleon is given by

$$\frac{d\sigma}{dE'd\omega_e d\Omega_\pi}=\frac{1}{2(2\pi)^5}\frac{E'}{E}\frac{QMm^2}{W}\times\tfrac{1}{4}\sum\left|\langle e'\pi N'|\frac{e}{k^2}j_\mu J_\mu|eN\rangle\right|^2,$$

where j_μ is the electron current operator given by quantum electrodynamics ($e^2/4\pi=\alpha$). That is,

$$\frac{d\sigma}{dE'd\omega_e d\Omega_\pi}=\frac{1}{2(2\pi)^5}\frac{E'}{E}\frac{QMm^2}{W}\frac{e^2}{k^4}[\tfrac{1}{2}\sum(\bar u_f\gamma_\mu u_i)(\bar u_f\gamma_\nu u_i)^*]\times[\tfrac{1}{2}\sum\langle\pi N'|J_\mu|N\rangle\langle\pi N'|J_\nu|N\rangle^*].$$

Working out the first bracket and abbreviating the second,

$$\frac{d\sigma}{dE'd\omega_e d\Omega_\pi}=\frac{1}{2(2\pi)^5}\frac{E'}{E}\frac{QMm^2}{W}\frac{e^2}{k^4}\frac{1}{2m^2}\times(r_\mu r_\nu'+r_\nu r_\mu'+\tfrac{1}{2}k^2g_{\mu\nu})T_{\mu\nu}. \tag{A4}$$

In the electron Breit frame, defined as the frame in which the electron scatters backward with no loss in energy, unpolarized relativistic electrons emit transverse unpolarized photons.[47] But in this frame we have

$$r_\mu r_\nu+r_\nu r_\mu+\tfrac{1}{2}k^2g_{\mu\nu}=-k^2e_{\mu\nu}, \tag{A5}$$

with $e_{xx}=e_{yy}=\frac{1}{2}$ and all other $e_{\mu\nu}=0$; that is, $e_{\mu\nu}$ is actually the density matrix of the virtual photon polarization. In the pion-nucleon center-of-mass frame the density matrix [removing a $(1-\epsilon)^{-1}$ normalization factor] becomes

$$\begin{aligned}
&e_{xx}=\tfrac{1}{2}(1+\epsilon),\ e_{yy}=\tfrac{1}{2}(1-\epsilon),\\
&e_{zz}=(K_0^2/-k^2)\epsilon,\\
&e_{tt}=(K^2M^2/-k^2W^2)\epsilon,\\
&e_{xz}=e_{zx}=[K_0/(-2k^2)^{1/2}][\epsilon(1+\epsilon)]^{1/2},\\
&e_{xt}=e_{tx}=[KM/(-2k^2)^{1/2}W][\epsilon(1+\epsilon)]^{1/2},\\
&e_{zt}=e_{tz}=(KK_0M/-k^2W)\epsilon,\\
&e_{xy}=e_{yx}=e_{yz}=e_{zy}=e_{y0}=e_{0y}=0,
\end{aligned} \tag{A6}$$

where $\epsilon=[2+(|\mathbf{k}|^2/-k^2)\tan^2(\frac{1}{2}\theta_e)]^{-1}$ is the transverse polarization, and the basis vectors $\hat x$, $\hat y$, and $\hat z$ are defined along $(\mathbf{K}\times\mathbf{R}')\times\mathbf{K}$, $\mathbf{K}\times\mathbf{R}'$, and $\mathbf{K}$, respectively. Combining (A1), (A4), and (A5) [with the $(1-\epsilon)^{-1}$ normalization factor], we can write

$$\frac{d\sigma}{dE'd\omega_e d\Omega_\pi}=\frac{e^2}{(2\pi)^3}\frac{E'}{E}\frac{|\mathbf{k}|}{-k^2}\frac{1}{1-\epsilon}\frac{d\sigma_v}{d\Omega_\pi}. \tag{A7}$$

The photoproduction cross section is labeled with v to emphasize that it is, in general, not equal to the $d\sigma/d\Omega_\pi$ measured in conventional photoproduction experiments. It is instead the differential cross section for pion production by a beam of virtual photons polarized as in (A6). Note that the polarization includes longitudinal and scalar components.

[46] Our argument parallels that of M. Gourdin, Nuovo Cimento 21, 1094 (1961). In Gourdin's work, however, the cross section is always averaged over ϕ.

[47] Since a relativistic electron preserves its helicity, the emitted photon is an equal incoherent mixture of $+1$ and -1 helicity states, that is unpolarized transverse. The idea of deducing the virtual photon polarization by starting in the Breit frame and transforming is due to L. N. Hand, Stanford University, Ph.D thesis, 1961 (unpublished).

C. Gauge Invariance

Our expression for the electron current assumes the Lorentz gauge, thus satisfying the condition $K_\mu j_\mu=0$. Gauge invariance then implies the same for the hadron current:

$$K_\mu J_\mu=0. \tag{A8}$$

Some models of the hadron vertex are not gauge invariant without some modification of the model. For instance, the relativistic Born approximation has $K_\mu J_\mu$ proportional to $k^2(F_\pi-F_{1v})$.[48] The most common technique for forcing gauge invariance adds a term proportional to K_μ to the hadron current. Gauge invariance uniquely determines the coefficient for this term. In practice, the addition is usually accomplished by projecting the amplitude onto six Lorentz invariants[23] which are manifestly gauge invariant. In the Lorentz gauge, all terms proportional to K_μ vanish in the product of the currents, so the result is equivalent to that obtained by ignoring the question of gauge invariance. This probably accounts for some of the popularity of the method.

If J_μ is gauge invariant, (A8) implies $\mathbf{K}\cdot\mathbf{J}=K_0J_0$; the longitudinal and scalar components are not independent. We can therefore simplify the expression for the virtual photoproduction cross section by eliminating the scalar (or longitudinal) component.[49] That is,

$$\begin{aligned} j_\mu J_\mu&=(\mathbf{K}\cdot\mathbf{j})(\mathbf{K}\cdot\mathbf{J})/K_0{}^2-\mathbf{j}\cdot\mathbf{J}\\ &=-j_xJ_x-j_yJ_y-(k^2/K_0{}^2)j_zJ_z. \end{aligned}$$

We can omit the scalar term in the amplitude provided we multiply the longitudinal term by $k^2/K_0{}^2$. To simplify the resulting formula we do this by multiplying the electron and hadron longitudinal currents each by $(-k^2)^{1/2}/K_0$ (with a minus sign in the hadron case). We can now replace (A6) by

$$e_{jk}=\begin{pmatrix} \frac{1}{2}(1+\epsilon) & 0 & [\frac{1}{2}\epsilon(1+\epsilon)]^{1/2}\\ 0 & \frac{1}{2}(1-\epsilon) & 0\\ [\frac{1}{2}\epsilon(1+\epsilon)]^{1/2} & 0 & \epsilon \end{pmatrix}, \tag{A9}$$

with the rows and columns labeled in x, y, z order. This is the density matrix corresponding to an equal incoherent mixture of two pure polarization states:

$$\begin{pmatrix} 0\\ [\frac{1}{2}(1-\epsilon)]^{1/2}\\ 0 \end{pmatrix} \quad\text{and}\quad \begin{pmatrix} [\frac{1}{2}(1+\epsilon)]^{1/2}\\ 0\\ (\epsilon)^{1/2} \end{pmatrix}. \tag{A10}$$

Substituting (A9) in (A1) and noting that $T_{\mu\nu}$ should be symmetric, we get the following expression for the virtual photoproduction cross section:

$$\frac{d\sigma_v}{d\Omega_\pi}=\frac{1}{4(2\pi)^2}\frac{M^2Q}{W^2K}\left[\frac{T_{xx}+T_{yy}}{2}+\epsilon\frac{T_{xx}-T_{yy}}{2}+\epsilon\frac{-k^2}{K_0{}^2}T_{zz}+[\epsilon(1+\epsilon)]^{1/2}\frac{[-2k^2]^{1/2}T_{xz}}{K_0}\right]. \tag{A11}$$

We note that the terms containing the longitudinal current (z subscripts) vanish in the limit $k^2=0$. If we had retained the scalar component instead of the longitudinal, Eq. (A11) would not be significantly different.

D. Azimuthal Dependence

Expressing $\mathbf{j}$ and $\mathbf{J}$ in terms of helicity states, we can write

$$\frac{d\sigma_v}{d\Omega_\pi}=\frac{1}{4(2\pi)^2}\frac{M^2Q}{W^2K}\left[\frac{T_{++}+T_{--}}{2}-\epsilon T_{+-}+\epsilon\frac{-k^2}{K_0{}^2}T_{00}+[\epsilon(1+\epsilon)]^{1/2}\frac{(-k^2)^{1/2}(T_{+0}-T_{-0})}{K_0}\right]. \tag{A12}$$

Since it represents the unpolarized transverse cross section, $(T_{++}+T_{--})$ does not depend on ϕ. Similarly, the longitudinal term T_{00} must be independent of ϕ. However, since T_{+-} comes from the interference between pion-nucleon states with l_z differing by two, it must contain the factor $\sin^2\Theta_\pi\cos2\phi$ and no other ϕ dependence. By a similar argument, the longitudinal-transverse interference term must contain the factor $\sin\Theta_\pi\cos\phi$.

We can now rewrite (A11) in the following form:

$$\begin{aligned} \frac{d\sigma_v}{d\Omega_\pi}(W,k^2,\epsilon,\Theta_\pi,\phi)&=A(W,k^2,\Theta_\pi)+\epsilon B(W,k^2,\Theta_\pi)\\ &\quad+\epsilon C(W,k^2,\Theta_\pi)\sin^2\Theta_\pi\cos2\phi\\ &\quad+[\epsilon(1+\epsilon)]^{1/2}D(W,k^2,\Theta_\pi)\sin\Theta_\pi\cos\Phi. \end{aligned} \tag{A13}$$

Equations (A7) and (A13) express the limit of our knowledge of the electroproduction cross section, based on quantum electrodynamics and the assumption of single-photon exchange. The explicit form of the four functions on the right-hand side of (A13) must be obtained from experiment or from a model of the off-mass-shell photoproduction process. The physical significance of the four functions is discussed in Sec. II.

APPENDIX II. RADIATIVE CORRECTIONS

The observed elastic scattering and electroproduction yields include radiative events in which the emitted photon does not perturb the momenta of the final electron (and pion) enough to prevent the event from

[48] Actually, since our data are consistent with $F_\pi=F_{1v}$, any ambiguities in the way one ensures gauge invariance have practically no effect on our results.

[49] R. H. Dalitz and D. R. Yennie, Phys. Rev. **105**, 1598 (1957). In theoretical calculations of $d\sigma_v/d\Omega_\pi$ it is generally more convenient to keep everything in covariant form until the end of the calculation.

being counted. In order to compare with theory it is customary to apply a correction factor $(1+\delta)^{-1}$ to the measured cross section to obtain an idealized cross section without radiation. The correction must take into account extra virtual photons as well as radiated real photons in order to avoid divergences. The real-photon part of the correction depends on the detection apertures, since these limit the range of photon momenta that will be counted.

Because of the large difference in masses, we may ignore radiation by the hadrons compared to radiation by the electrons. The similarity of the electron currents in elastic and inelastic scattering then makes the form of the radiative correction the same for each. In elastic scattering the electron momentum at a given angle is constrained by two-body kinematics. In electroproduction the detection of the pion at fixed momentum and angle imposes an analogous constraint on the electron momentum. Therefore, the aperture-dependent parts of the radiative corrections for elastic scattering and electroproduction are quite similar provided the same electron spectrometer is used in both measurements.

Making the peaking approximation in the evaluation of the radiation probability, we obtain

$$\delta_e=\frac{\alpha}{\pi}\left\{\frac{13}{6}\ln\left(\frac{-k^2}{m^2}\right)-\frac{28}{9}+\left[\ln\left(\frac{-k^2}{m^2}\right)-1\right]\times\ln\left[\frac{E}{E'}\left(\frac{\Delta E'}{E'}\right)^2\right]\right\}$$

for the correction to the elastic cross section, and

$$\delta_{e\pi}=\frac{\alpha}{\pi}\left\{\frac{13}{6}\ln\left(\frac{-k^2}{m^2}\right)-\frac{28}{9}+\left[\ln\left(\frac{-k^2}{m^2}\right)-1\right]\times\ln\left[\frac{dE'}{dE}\left(\frac{W}{M}\right)^2\left(\frac{E^2}{E}\right)^2\left(\frac{\Delta E'}{E'}\right)^2\right]\right\}$$

for the electroproduction correction (E' and k^2 are not the same in corresponding measurements though). These corrections agree within 0.02 with more accurate calculations.[50] For our data $\delta=-0.10$ typically. The net effect of the radiative correction on the measured ratio of electroproduction and elastic scattering was never more than 2%. We have ignored both corrections and have estimated the contribution to the error in the ratio to be $\pm 2\%$.

[50] For the correction to elastic scattering see N. Meister and D. R. Yennie, Phys. Rev. 130, 1210 (1963); for the electroproduction correction see A. Bartl and P. Urban, Acta Phys. Austriaca 24, 139 (1966).

PHYSICAL REVIEW VOLUME 163, NUMBER 5 25 NOVEMBER 1967

Determination of the S-Wave $\pi\pi$ Phase Shifts in the ρ Region from 4.16-GeV/c π^-p Interactions*

P. B. JOHNSON, L. J. GUTAY, R. L. EISNER, P. R. KLEIN, R. E. PETERS, R. J. SAHNI, W. L. YEN, AND G. W. TAUTFEST
Department of Physics, Purdue University, Lafayette, Indiana
(Received 19 July 1967)

The results of a calculation of the $T=0$ and $T=2$ S-wave $\pi\pi$ elastic scattering phase shifts in the ρ region are presented. Two solutions are found for both. One set for δ_0^0 does not pass through 90°. The physically acceptable solution for the δ_0^2 phase shift is found to be small ($|\delta_0^2|<20°$). The absorption corrections are essential for the determination of δ_0^0.

IN this paper, we present the results of a calculation of the $I=0$ and $I=2$ S-wave $\pi\pi$ elastic scattering phase shifts based on a method reported previously.[1] The motivation for this investigation has been to include the effects of an $I=2$, S-wave amplitude and to test the consistency of the model at a different incident momentum. The data is taken from two-prong π^-p interactions at an incident pion momentum of 4.16 GeV/c from an exposure of the Lawrence Radiation Laboratory 72-in. hydrogen bubble chamber. The two reactions considered are

$$\pi^-p\rightarrow\pi^+\pi^-n, \quad (1)$$

$$\pi^-p\rightarrow\pi^0\pi^-p. \quad (2)$$

The sample consists of approximately 4400 events from reaction (1) and 2900 events from reaction (2). The selection of these events and other details about this experiment are discussed elsewhere.[2]

The absorption-modified one-pion-exchange model has been quite successful in predicting the differential

* Work supported in part by U. S. Atomic Energy Commission.
[1] L. J. Gutay, P. B. Johnson, F. J. Loeffler, R. L. McIlwain, D. H. Miller, R. B. Willmann, and P. L. Csonka, Phys. Rev. Letters 18, 142 (1967).

[2] R. L. Eisner, P. B. Johnson, P. R. Klein, R. E. Peters, R. J. Sahni, W. L. Yen, and G. W. Tautfest, Phys. Rev. (to be published).